Semiconductor Physics, Quantum Electronics & Optoelectronics, 2024. V. 27, No 3. P. 280-286.

Semiconductor physics

Particularities of optical behavior of Ag_8SiS_6 single crystal

A.I. Pogodin[1*], I.O. Shender[1], M.M. Pop[1], M.J. Filep[1,2], T.O. Malakhovska[1], O.P. Kokhan[1], V.Yu. Izai[3], R. Mariychuk[4]

[1]*Uzhhorod National University, 46, Pidgirna str., 88000 Uzhhorod, Ukraine*
[2]*Ferenc Rákóczi II Transcarpathian Hungarian Institute, Kossuth Sq. 6, 90200 Beregovo, Ukraine*
[3]*Comenius University, Mlynska dolina, Bratislava 84248, Slovakia*
[4]*University of Presov, 17th November 1, Presov 08116, Slovakia*
[*]*Corresponding author e-mail: artempogodin88@gmail.com*

Abstract. Ag_8SiS_6 single crystal was grown by directional crystallization from melt. A crystal sample was investigated by optical ellipsometry and spectroscopy. This sample had nonlinear spectral dependences of the refractive index *n* and the extinction coefficient *k*. The presence of a sharp maximum in the spectral dependence of the refractive index and a rather sharp decrease in the values of the extinction coefficient *k* at the wavelength of 780 nm were found. The behavior of the optical absorption edge of the Ag_8SiS_6 single crystal in the temperature range of 77…300 K was studied. An exponential dependence of the absorption coefficient α obeying the Urbach rule was observed at all the investigated temperatures. The optical pseudo-gap E_g^* and the Urbach energy E_U were calculated from the obtained experimental data. An increase in temperature of the Ag_8SiS_6 crystal was found to lead to a monotonic, almost linear decrease in E_g^* (1.853…1.615 eV) and a monotonic nonlinear increase in E_U (44.32…55.01 meV). The contributions of the temperature-independent $(E_U)_{X,C}$ and temperature-dependent $(E_U)_T$ components to the total Urbach energy E_U for Ag_8SiS_6 were evaluated within the Einstein model.

Keywords: argyrodite, single crystal, optical absorption edge, Urbach's rule.

https://doi.org/10.15407/spqeo27.03.280
PACS 07.60.Fs, 78.20.Ci

Manuscript received 01.05.24; revised version received 15.07.24; accepted for publication 11.09.24; published online 20.09.24.

1. Introduction

Study of optical properties of materials is an important field of both optics and materials science as well as relevant for a large number of scientific and technical fields, including solid-state physics, crystallography, photonics, nanotechnology, and others. These studies allow us to establish relationships between the structure and optical characteristics of the materials under study, which are key for developing new materials with improved optical properties or for optimizing existing materials for specific applications [1–4]. Understanding optical properties and their possible applications is crucial for developing new optical devices and systems [5, 6].

Ternary and more complex silver-based compounds belong to potential optical materials [7–11], which are characterized by wide wave operating regions. Among these compounds, complex sulfides called argyrodites have attracted considerable interest in recent years as perspective optical materials [12, 13]. They have an optimal band gap energy according to the Shockley–Queisser limit [14]. Argyrodite (Ag_8GeS_6) and canfieldite (Ag_8SnS_6) nanocrystals are characterized by E_g in the range of 1.24…1.41 eV [13, 15]. Possible applications of $Ag_8Ge(Sn)S_6$-based materials include light absorbers in thin film solar cells and photoanodes for photoelectrochemical water splitting.

A defining characteristic of argyrodites is the presence of a disordered cationic sublattice within the voids formed by the ordered tetrahedral dense packing [16–18]. This causes the appearance of the so-called Urbach tails, *i.e*. the fundamental optical absorption edge has an exponential shape (Urbach's rule) [19, 20]. Investigation of the absorption edge behavior in a wide temperature range allows one to determine the parameters that influence the mechanism of light absorption. Moreover, a detailed study of the temperature dependence of the band gap values extends practical applications of the materials.

In this study, Ag_8SiS_6, a selenium-containing analog of canfieldite, was chosen for the study. Ag_8SiS_6 crystal has a primitive orthorhombic cell with the cell parameters

a = 15.065 Å, b = 7.439 Å, c = 10.545 Å and Z = 4 and belongs to the space group $Pna2_1$ [21]. As is typical for all ternary argyrodites, Ag_8SiS_6 undergoes structural phase transition ($Pna2_1 \leftrightarrow$ F-43m) at 513 K [21].

This work is aimed at the study and modeling of spectral dependence of dispersion of refractive index and temperature dependence of optical transmission spectra of single crystalline Ag_8SiS_6 samples.

2. Experimental

2.1. Materials and methods

20 g of Ag_8SiS_6 were synthesized from elemental high-purity Ag (99.995%), Si (99.9999%), and S (99.999%) taken in stoichiometric ratios, in a quartz ampoule evacuated to 0.13 Pa. The synthesis regime included heating to 450 °C at a rate of 50 °C/h and keeping at this temperature for 48 hours to ensure interaction of all the sulfur with silver and silicon. After the exposure, the synthesis temperature was increased to 1015 °C (50 °C above the Ag_8SiS_6 melting point) at a rate of 50 °C/h, and the melt was kept at this temperature for 72 hours. After completion of the chemical interaction, the Ag_8SiS_6 melt was cooled down to room temperature at the rate 50 °C/h. As a result of the synthesis, a dark gray polycrystalline alloy was obtained. It was transferred to a special quartz ampoule for the growth of the single crystal.

Ag_8SiS_6 single crystal was grown by directional crystallization from the melt in an evacuated quartz ampoule placed in a two-temperature tube furnace with independent control of each zone. The temperatures in the melt (upper) and annealing (lower) zones were 1015 °C and 640 °C, respectively. The crystallization front was moved at a rate of 0.5 mm/h. The Ag_8SiS_6 single crystal was annealed for 72 h in the lower zone to relieve thermal stresses and then cooled down to room temperature at a rate of 5 °C/h. As a result, a single crystal of dark gray color with a metallic luster, 4 cm long and 1.2 cm in diameter was obtained.

The refractive index n and extinction coefficient k of the Ag_8SiS_6 single crystal were studied using a Horiba Smart SE spectral ellipsometer in the spectral range of 440…1000 nm at an incidence angle of 70°. The obtained experimental results were analyzed with the DeltaPsi2 software using the Tauc–Lorenz model [22, 23].

Optical transmission spectra were measured in the spectral range of 450…1100 nm at temperatures of 77…300 K using a LOMO KSVU-23 grating monochromator (resolution ~ 1 Å). The value of the absorption coefficient α was calculated according to the known formula (Eq. (1)) based on the experimental transmittance spectrum T' [24, 25]:

$$\alpha = \frac{1}{d}\ln\left[\frac{(1-R)^2 + \sqrt{(1-R)^4 + 4T'^2R^2}}{2T'}\right], \quad (1)$$

where d is the sample thickness and R is the specular reflection coefficient, respectively.

The specular reflection coefficient R was calculated (Eq. (2)) from the spectral dependence of the refractive index according to the well-known Fresnel equation [25] for normal incidence:

$$R = \left(\frac{n_1 - 1}{n_1 + 1}\right)^2. \quad (2)$$

3. Results and discussion

The spectral dependences of the refractive index n and the extinction coefficient k (Fig. 1) were found to be non-monotonic and non-linear. This is demonstrated by the presence of a sharp maximum on the spectral dependence of the refractive index n and a rather sharp decrease in the values of the extinction coefficient k (Fig. 1) at 780 nm (1.586 eV). It should be noted that the spectral region of λ < 780 nm corresponds to the optical absorption edge of Ag_8SiS_6. It is noteworthy that in the longer-wavelength region, *i.e.*, in the transparency region of Ag_8SiS_6, the values of the refractive index and the extinction coefficient are characterized by a tendency to a sharp (n) and monotonous (k) decrease (Fig. 1).

The spectral dependence of the refractive index is well described by the Wemple–DiDomenico model (Eq. (3)) [26]:

$$n^2(E) - 1 = \frac{E_d^{WD} E_0^{WD}}{\left(E_0^{WD}\right)^2 - E^2}, \quad (3)$$

where E_0^{WD} is the energy of a single oscillator and E_d^{WD} is the dispersion energy, respectively.

The Wemple–DiDomenico model describes the dispersion of the refractive index based on the relationship between the refractive index and the width of the pseudo-gap. This model is used to explain the peculiarities of the dispersion of the refractive index in the transparency region of the material. It should be noted that the parameters of the Wemple–DiDomenico model are important for understanding and modeling the behavior of semiconductor devices and are used to optimize their characteristics [26].

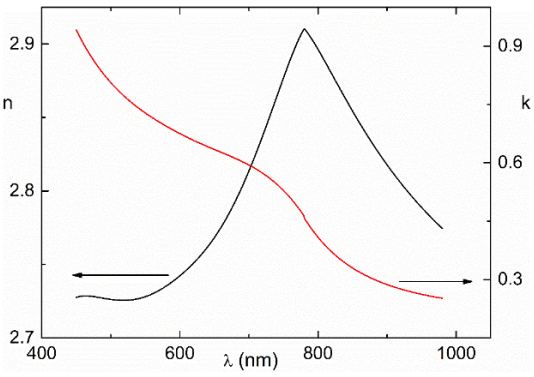

Fig. 1. Spectral dependences of refractive index n and extinction coefficient k of Ag_8SiS_6.

As a result of the analysis (Eq. (3)), the single oscillator energy value E_0^{WD} was found to be 3.24 eV, and the dispersion energy E_d^{WD} to be 17.7 eV. The latter parameter characterizes the average energy of interband optical transitions and may be related to changes in the structural order/disorder of the material (ionicity, anion valence and coordination number). It is known [27] that the energy of a single oscillator E_0^{WD} is related to the value of the band gap E_g by the ratio $E_0^{WD} \approx 2E_g^{WD}$. Therefore, the value of the band gap E_g^{WD} for Ag_8SiS_6 estimated by this ratio is ~ 1.62 eV.

Using the Wemple–DiDomenico model and Eqs. (4) and (5), the value of the static refractive index n_0^{WD} was found to be 2.57, and the value of f_i^{WD}, which is responsible for the ionicity of the material, is 0.65:

$$n_0^{WD} = \left[1 + \frac{E_d^{WD}}{E_0^{WD}}\right]^{\frac{1}{2}}, \quad (4)$$

$$f_i^{WD} = \left[\frac{E_0^{WD}}{E_d^{WD}}\right]^{\frac{1}{2}}. \quad (5)$$

It was found that in the entire studied temperature range, the energy dependences of ln α in the optical absorption edge region are exponential (Fig. 2), indicating that they obey the Urbach rule [24, 28]:

$$\alpha(h\nu, T) = \alpha_0 \exp\left[\frac{h\nu - E_0}{E_U(T)}\right]. \quad (6)$$

Here, α_0 and E_0 are the coordinates of the convergence point of the Urbach "bundle", $h\nu$ and T are the photon energy and temperature, respectively, and $E_U(T)$ is the Urbach energy.

An increase in temperature was found to lead to a shift in the spectral dependences towards shorter wavelengths (Fig. 2), which indicates a decrease in the E_g value. However, given the nature of the ln α($h\nu$) dependences, it is only possible to discuss the optical pseudo-band gap E_g^*, which is associated with a "blurred" optical absorption edge, *i.e.*, absence of clear linear areas in the absorption edge region. This blurring is caused by masking of direct optical absorption transitions by low-energy (long-wave) Urbach tails. The authors [29] proved that using of the value of the pseudo-gap energy E_g^* instead of the band gap energy E_g is quite correct in this case. As a result, the value of the pseudo-gap energy E_g^* is taken at a fixed value of the absorption coefficient α equal to 10^3 cm^{-1}.

It should be noted that extrapolation of the linear (high-energy) sections of the ln α($h\nu$) dependences indicates the presence of one intersection point with the coordinates α_0 and E_0 and leads to the appearance of a well-known Urbach "bundle" (Fig. 2). This behavior indicates the absence of phase transitions in Ag_8SiS_6 in the studied temperature range and the same mechanism of electron-phonon interaction (EPI).

Applying Eq. (6) to the optical absorption spectra (Fig. 2), we calculated (Table 1) the values of the pseudo-gap energy E_g^*, the Urbach energy E_U (parameter of optical absorption edge blurring), and the optical absorption edge steepness parameter σ that is related to EPI by the Mahr formula [28]:

$$\sigma(T) = \sigma_0 \left[\frac{2kT}{\eta\omega_p}\right] \cdot \tanh\left[\frac{\eta\omega_p}{2kT}\right], \quad (7)$$

where $\hbar\omega_p$ is the effective average phonon energy in a single oscillator model, k is the Boltzmann constant, and σ_0 is the parameter related to the EPI constant g as $\sigma_0 = 2/3g$.

It should be noted that if the parameters σ and σ_0 are smaller than 1, EPI is strong [30], and the smaller they are, the stronger EPI is.

It was found that an increase in temperature leads to a monotonic increase in the parameter σ (Fig. 3), which indicates weakening of EPI. But regardless of this, EPI is strong in the entire temperature range under study. It is important to consider the temperature dependence of the pseudo-gap E_g^* and the Urbach energy E_U, as illustrated in Fig. 4.

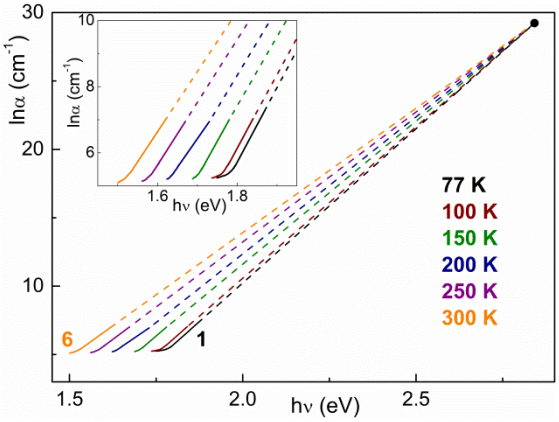

Fig. 2. Energy dependences of the logarithm of the absorption coefficient for Ag_8SiS_6 single crystal in the temperature range from 77 K (*1*) to 300 K (*6*).

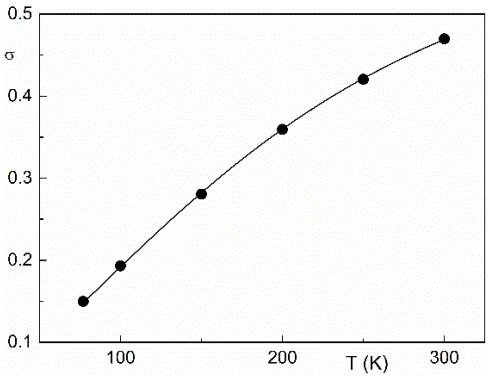

Fig. 3. Temperature dependence of the optical absorption edge steepness parameter σ.

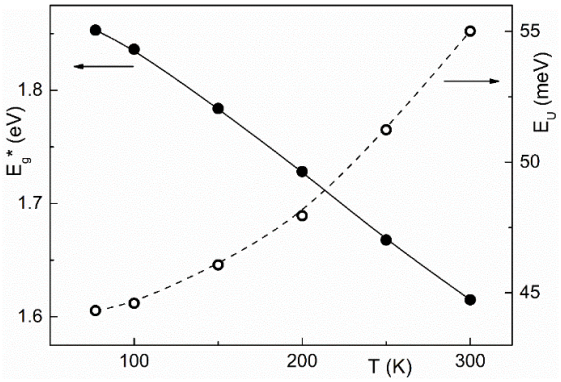

Fig. 4. Temperature dependences of the pseudo-gap E_g^* and the Urbach energy E_U for Ag_8SiS_6 crystal.

An increase in temperature leads to a monotonic, almost linear decrease in the values of the pseudo-gap E_g^* (1.853…1.615 eV) and a monotonic nonlinear increase in the Urbach energy E_U (44.32…55.01 meV) (Fig. 4) for the Ag_8SiS_6 crystal. The latter indicates that an increase in temperature increases the disorder in the Ag_8SiS_6 structure. It should be noted that the temperature dependences of σ, E_g^* and E_U are well consistent with each other. The change in these parameters is primarily due to the temperature-stimulated increase in the amplitude of atomic vibrations in the crystal structure of Ag_8SiS_6. This can lead to an increase in the volume and deformation of the structure-forming polyhedra, which causes an increase in the unit cell parameters of the Ag_8SiS_6 and weakens interatomic interactions as a consequence. As a result, the electron density of local hybridized atomic orbitals is redistributed and their energy level in the electronic structure is blurred. Due to this, the decrease in the EPI (Fig. 3), the increase in the Urbach energy, and the decrease in the pseudo-gap (Fig. 4) with temperature are observed.

The temperature dependences of the pseudo-gap E_g^* and the Urbach energy E_U were described using Einstein's relations, which allowed us to determine the values of the parameters $E_g^*(0)$, S_g^*, θ_E, $(E_U)_0$ and $(E_U)_1$ (Table) [31, 32]:

$$E_g^*(T) = E_g^*(0) - S_g^* k\theta_E \left[\frac{1}{\exp(\theta_E/T)-1}\right], \quad (8)$$

$$E_U(T) = (E_U)_0 - (E_U)_1 \left[\frac{1}{\exp(\theta_E/T)-1}\right], \quad (9)$$

where S_g^* is the dimensionless constant, θ_E is the Einstein temperature, and $(E_U)_0$ and $(E_U)_1$ are the constants, respectively.

It was shown in [33] that the Urbach energy E_U is related to the temperature and structural disorder, which ultimately affect the shape (blurring) of the optical absorption edge described by the following relation:

$$E_U = (E_U)_T + (E_U)_X + (E_U)_C = (E_U)_T + (E_U)_{X+C}. \quad (10)$$

Table. Optical absorption edge and EPI parameters for Ag_8SiS_6 single crystal at 300 K.

α_0 (cm^{-1})	E_0 (eV)	E_g^* (eV)	E_U (meV)	σ_0	$\hbar\omega_p$ (meV)
4.93 10^{12}	2.84	1.615	55.01	0.66	58.79

θ_E (K)	$(E_U)_0$ (meV)	$(E_U)_1$ (meV)	$E_g^*(0)$ (eV)	S_g^*
214.60	43.60	7.80	1.87	14.97

Here, $(E_U)_T$, $(E_U)_X$ and $(E_U)_C$ are respectively the contributions of temperature, structural and compositional disorder to the Urbach energy E_U [33].

The temperature and structural contributions $(E_U)_T$ and $(E_U)_{X+C}$ to the total Urbach energy E_U are independent, which means that the total Urbach energy can be expressed as the sum of the temperature and structural contributions. The origin of the temperature disorder is described above. The structural disorder includes the presence of additional defects in the crystal structure, such as dislocations, vacancies, *etc*., as well as microstructural defects, such as microcracks, planar defects, and small-angle boundaries. The latter can appear due to phase transformations. It is known [21] that Ag_8SiS_6 is characterized by a high-temperature (240 °C) F-43m↔$Pna2_1$ phase transformation. Therefore, it is not surprising that the structure-dependent contribution $(E_U)_{X+C}$ to the total Urbach energy E_U of Ag_8SiS_6 is dominant and amounts to 79%.

4. Conclusions

The optical properties of the Ag_8SiS_6 single crystal have been studied by spectral ellipsometry and optical spectroscopy. The refractive index dispersion is demonstrated to have a maximum coinciding with the optical absorption edge and is well described by the Wemple–DiDomenico model. The optical absorption edge of the studied Ag_8SiS_6 in the temperature range of 77…300 K has an exponential shape and corresponds to Urbach's rule. The temperature behavior of the Urbach absorption edge is determined by EPI, which is quite strong in Ag_8SiS_6 crystals.

The temperature dependences of the optical pseudo-gap E_g^* and the Urbach energy E_U have been experimentally obtained. They are well described in the framework of the Einstein model. A shift of the optical absorption edge towards high energies and a decrease of the Urbach energy are observed at decreasing temperature. Contributions of the temperature-independent $(E_U)_{X,C}$ and temperature-dependent $(E_U)_T$ components to the total Urbach energy E_U for Ag_8SiS_6 are evaluated within the Einstein model. The blurring of the optical absorption edge is found to be mainly due to the contribution of static structural disorder to the Urbach energy (79%) as compared to the contribution of the temperature component.

Acknowledgements

This work was supported by the grants of the National Scholarship Programme of the Slovak Republic [Grant ID: 52200 and Grant ID: 52201].

The authors also thank the Armed Forces of Ukraine for providing security to perform this work. This work has become possible only because of the resilience and courage of the Ukrainian Army.

References

1. Olley J.A. Structural disorder and the Urbach edge. *Solid State Commun*. 1973. **13**. P. 1437–1440. https://doi.org/10.1016/0038-1098(73)90184-1.
2. Studenyak I.P., Kayla M.I., Kranjčec M. *et al*. Isoabsorption and spectrometric studies of optical absorption edge in Cu_6AsS_5I superionic crystal. *J. Phys. Chem. Solids*. 2011. **72**. P. 1419–1422. https://doi.org/10.1016/j.jpcs.2011.08.012.
3. Sangiorgi N., Aversa L., Tatti R. *et al*. Spectrophotometric method for optical band gap and electronic transitions determination of semiconductor materials. *Opt. Mater*. 2017. **64**. P. 18–25. https://doi.org/10.1016/j.optmat.2016.11.014.
4. Ledinsky M., Schönfeldová T., Holovský J. *et al.* Temperature dependence of the Urbach energy in lead iodide perovskites. *J. Phys. Chem. Lett*. 2019. **10**. P. 1368–1373. https://doi.org/10.1021/acs.jpclett.9b00138.
5. Kumbhakar P., Gowda C.C., Tiwary C.S. Advance optical properties and emerging applications of 2D materials. *Front. Mater.* 2021. **8**. P. 291. https://doi.org/10.3389/fmats.2021.721514.
6. Singh J. *Optical Properties of Materials and Their Applications*. John Wiley & Sons Ltd., 2019. https://doi.org/10.1002/9781119506003.
7. Larsen J.K., Donzel-Gargand O., Sopiha K.V. *et al.* Investigation of $AgGaSe_2$ as a wide gap solar cell absorber. *ACS Appl. Energy Mater*. 2021. **4**. P. 1805–1814. https://doi.org/10.1021/acsaem.0c02909.
8. Daniel T., Henry J., Mohanraj K., Sivakumar G. $AgSbS_2$ and Ag_3SbS_3 absorber materials for photovoltaic applications. *Mater. Chem. Phys*. 2016. **181**. P. 415–421. https://doi.org/10.1016/j.matchemphys.2016.06.077.
9. Ju M.-G., Dai J., Ma L., Zhou Y., Zeng X.C. $AgBiS_2$ as a low-cost and eco-friendly all-inorganic photovoltaic material: nanoscale morphology–property relationship. *Nanoscale Adv*. 2020. **2**. P. 770–776. http://doi.org/10.1039/C9NA00505F.
10. Vu T.V., Khyzhun O.Y., Lavrentyev A.A. *et al.* Highly anisotropic layered crystal $AgBiP_2Se_6$: Growth, electronic band-structure and optical properties. *Mater. Chem. Phys*. 2022. **277**. P. 125556. https://doi.org/10.1016/j.matchemphys.2021.125556.
11. Bousselmi G., Khemiri N., Kanzari M. A new route for the synthesis of *n*-type Ag_2ZnSnS_4 thin films by thermal vacuum evaporation for solar cell applications. *Opt. Mater*. 2022. **134A**. P. 113187. https://doi.org/10.1016/j.optmat.2022.113187.
12. Boon-on P., Aragaw B.A., Lee C.-Y. *et al.* Ag_8SnS_6: a new IR solar absorber material with a near optimal bandgap. *RSC Adv*. 2018. **8**. P. 39470–39476. https://doi.org/10.1039/C8RA08734B.
13. Li Z., Liu C., Zhang X. *et al.* An easily prepared Ag_8GeS_6 nanocrystal and its role on the performance enhancement of polymer solar cells. *Org. Electron*. 2017. **45**. P. 247–255. https://doi.org/10.1016/j.orgel.2017.03.029.
14. Sutherland B.R. Solar materials find their band gap. *Joule*. 2020. **4**. P. 984–985. https://doi.org/10.1016/j.joule.2020.05.001.
15. Chowdhury A.P., Shambharkar B.H. BiOBr-Ag_8SnS_6 heterostructured nanocomposite photocatalysts: Synthesis, characterization, and photocatalytic application. *Asia-Pac. J. Chem. Eng.* 2018. **13**. P. e2182. https://doi.org/10.1002/apj.2182.
16. Kuhs W.F., Nitsche R., Scheunemann K. The argyrodites – a new family of tetrahedrally close-packed structures. *Mat. Res. Bull*. 1979. **14**. P. 241–248. https://doi.org/10.1016/0025-5408(79)90125-9.
17. Pogodin A.I., Filep M.J., Studenyak V.I. *et al.* Influence of crystal structure disordering on ionic conductivity of $Ag_{7+x}(P_{1-x}Ge_x)S_6$ single crystals. *J. Alloys Compd.* 2022. **926**. P. 166873. https://doi.org/10.1016/j.jallcom.2022.166873.
18. Nilges T., Pfitzner A. A structural differentiation of quaternary copper argyrodites: Structure – property relations of high temperature ion conductors. *Z. Kristallogr*. 2005. **220**. P. 281–294. https://doi.org/10.1524/zkri.220.2.281.59142.
19. Zeiske S., Sandberg O.J., Zarrabi N. *et al.* Static disorder in lead halide perovskites. *J. Phys. Chem. Lett*. 2022. **13**. P. 7280–7285. https://doi.org/10.1021/acs.jpclett.2c01652.
20. Banik I., Lukovičová J., Pavlendová G., Podoba R. Some open problems in physics of disordered materials (and their possible solutions on the base of the barrier-cluster-heating model). *AIP Conf. Proc.* 2013. **1564**. P. 117–122. https://doi.org/10.1063/1.4832805.
21. Pogodin A., Filep M., Malakhovska T. *et al.* Obtaining of disordered highly ionic conductive $Ag_{7+x}(P_{1-x}Si_x)S_6$ single crystalline materials. *Mater. Res. Bull*. 2024. **179**. P. 112953. https://doi.org/10.1016/j.materresbull.2024.112953.
22. Jellison G.E., Modine F.A. Parameterization of the optical functions of amorphous materials in the interband region. *Appl. Phys. Lett*. 1996. **69**. P. 371–373. https://doi.org/10.1063/1.118064.
23. Fujiwara H. *Spectroscopic Ellipsometry. Principles of Spectroscopic Ellipsometry*. John Wiley & Sons. 2007. https://doi.org/10.1002/9780470060193.
24. Urbach F. The long-wavelength edge of photographic sensitivity and electronic absorption of solids. *Phys. Rev*. 1953. **92.** P. 1324–1326. https://doi.org/10.1103/PhysRev.92.1324.

25. Skaar J. Fresnel equations and the refractive index of active media. *Phys. Rev. E*. 2006. **73**. P. 026605. https://doi.org/10.1103/physreve.73.026605.
26. Wemple S.H., Di Domenico M. Behaviour of the dielectric constant in covalent and ionic materials. *Phys. Rev. B.* 1971. **3**. P. 1338–1352. https://doi.org/10.1103/PhysRevB.3.1338.
27. Tanaka K. Optical properties and photoinduced changes in amorphous As-S films. *Thin Solid Films*. 1980. **66**. P. 271–279. https://doi.org/10.1016/0040-6090(80)90381-8.
28. Kurik M.V. Urbach rule (review). *phys. status solidi* (*a*). 1971. **8**. P. 9−30. https://doi.org/10.1002/pssa.2210080102.
29. Studenyak I.P., Kranjčec M., Kovács Gy.S. *et al.* Fundamental optical absorption edge and exciton–phonon interaction in Cu_6PS_5Br superionic ferroelastic. *Mater. Sci. Eng.: B.* 1998. **52**. P. 202–207. https://doi.org/10.1016/S0921-5107(97)00278-X.
30. Sumi H., Sumi A. The Urbach–Martiensen rule revisited. *J. Phys. Soc. Jpn*. 1987. **56**. P. 2211–2220. https://doi.org/10.1143/JPSJ.56.2211.
31. Beaudoin M., DeVries A.J.G., Johnson S.R. *et al.* Optical absorption edge of semi-insulating GaAs and InP at high temperatures. *Appl. Phys. Lett*. 1997. **70**. P. 3540–3542. https://doi.org/10.1063/1.119226.
32. Yang Z., Homewood K.P., Finney M.S. *et al.* Optical absorption study of ion beam synthesized polycrystalline semiconducting $FeSi_2$. *J. Appl. Phys.* 1995. **78**. 1958–1963. https://doi.org/10.1063/1.360167.
33. Cody G.D., Tiedje T., Abeles B. *et al.* Disorder and the optical-absorption edge of hydrogenated amorphous silicon. *Phys. Rev. Lett*. 1981. **47**. P. 1480. https://doi.org/10.1103/PhysRevLett.47.1480.

Authors and CV

Artem I. Pogodin, defended his PhD thesis in Inorganic Chemistry in 2016. Senior Researcher at the Uzhhorod National University. Authored over 100 scientific papers and 114 patents. The area of his scientific interests includes solid state chemistry, crystal growth and materials science.
https://orcid.org/0000-0002-2430-3220

Iryna O. Shender, defended her PhD thesis in Applied Physics and Nanomaterials at the Uzhhorod National University, Faculty of Physics in 2024. Authored 32 scientific papers and 7 patents. The area of her scientific interests is electrical, optical and mechanical properties of superionic conductors.
E-mail: shender95@gmail.com,
https://orcid.org/0000-0003-1687-3634

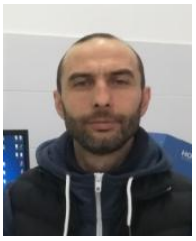

Mykhailo M. Pop, defended his PhD thesis in Physics and Mathematics in 2016. Lecturer and Researcher at the Uzhhorod National University. Authored of nearly 100 publications. The area of his scientific interests includes physical and optical properties of semiconductors, superionic materials, chalcogenide glasses and films.
E-mail: mykhaylo.pop@uzhnu.edu.ua,
https://orcid.org/0000-0003-3674-3482

Mykhailo J. Filep, PhD in Inorganic Chemistry, Senior Researcher at the Uzhhorod National University, Associate Professor at the Ferenc Rákóczi II Transcarpathian Hungarian Institute. Authored over 100 scientific papers and 50 patents. The area of his scientific interests includes solid state chemistry and materials science.
E-mail: mfilep23@gmail.com,
http://orcid.org/0000-0001-7017-5437

Tetyana O. Malakhovska, defended her PhD thesis in Inorganic Chemistry in 2010. Senior Researcher at the Uzhhorod National University. Authored 70 scientific papers and 10 patents. The area of her scientific interests includes solid state chemistry and materials science.
E-mail: t.malakhovska@gmail.com,
https://orcid.org/0000-0001-7309-4894

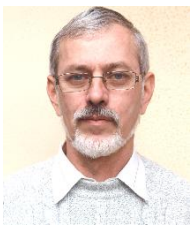

Oleksandr P. Kokhan, PhD, Associate Professor at the Inorganic Chemistry Department, Uzhhorod National University. Authored over 80 scientific papers and 95 patents. The area of his scientific interests includes inorganic chemistry, solid state chemistry, crystal growth, and materials science. E-mail: aleksandr.kokh@gmail.com,
http://orcid.org/0000-0003-1534-6779

Ruslan Mariychuk, PhD, Associate Professor at the Department of Ecology, University of Presov, Slovakia. Author of over 60 publications indexed in Scopus and Web of Science databases and 3 patents. His research interests include green chemistry, sustainable synthesis of nanomaterials, and materials science.
E-mail: ruslan.mariychuk@unipo.sk,
https://orcid.org/0000-0001-8464-4142

Vitalii Yu. Izai, PhD in Physics of Semiconductors and Dielectrics. Senior Researcher at the Uzhhorod National University until 2017. Scientific Associate at the Faculty of Mathematics, Physics and Informatics, Comenius University Bratislava since 2017. Authored 40 scientific papers and more than 20 patents (1 in the EU database). The area of his scientific interests includes materials science, superionic materials for solid-state ionics, deposition and physical properties of thin films obtained using various plasma enhanced PVD and CVD techniques, and design of artificial materials and interfaces. E-mail: vitalii.izai@fmph.uniba.sk, https://orcid.org/0000-0001-7512-3388

Authors' contributions

Pogodin A.I.: conceptualization, investigation, supervision, writing – original draft.
Shender I.O.: investigation, writing – original draft.
Pop M.M.: methodology, investigation, writing – original draft.
Filep M.J.: investigation, visualization, writing – review & editing..
Malakhovska T.O.: methodology, writing – review & editing.
Kokhan O.P.: investigation, writing – original draft.
Izai V.: methodology, investigation.
Mariychuk R.: methodology, writing – review & editing.

Особливості оптичної поведінки монокристала Ag_8SiS_6

А.І. Погодін, І.О. Шендер, М.М. Поп, М.Й. Філеп, Т.О. Малаховська, О.П. Кохан, В.Ю. Ізай, Р. Марійчук

Анотація. Монокристал Ag_8SiS_6 було вирощено методом спрямованої кристалізації з розплаву. Кристалічний зразок Ag_8SiS_6 було досліджено методами оптичної еліпсометрії та спектроскопії. Спектральні залежності показника заломлення n і коефіцієнта екстинкції k зразка мають нелінійний характер. Було встановлено наявність різкого максимуму в спектральній залежності показника заломлення і різке зменшення значень коефіцієнта екстинкції k при довжині хвилі 780 нм. Було досліджено поведінку краю оптичного поглинання монокристала Ag_8SiS_6 у температурному інтервалі 77…300 K. При всіх досліджених температурах спостерігалася експоненціальна залежність коефіцієнта поглинання α, яка підпорядковується правилу Урбаха. З отриманих експериментальних даних було розраховано оптичну псевдоширину забороненої зони E_g^* та енергію Урбаха E_U. Було встановлено, що для монокристала Ag_8SiS_6 підвищення температури приводить до монотонного, майже лінійного зменшення E_g^* (1.853…1.615 еВ) та монотонного нелінійного збільшення E_U (44.32…55.01 меВ). В рамках моделі Ейнштейна було оцінено внесок температурно-незалежної $(E_U)_{X,C}$ і температурно-залежної $(E_U)_T$ компонент у повну енергію Урбаха E_U для Ag_8SiS_6.

Ключові слова: аргіродит, монокристал, край оптичного поглинання, правило Урбаха.